

RESEARCH ARTICLE

Starvation induces FoxO-dependent mitotic-to-endocycle switch pausing during *Drosophila* oogenesis

Patrick Jouandin^{1,2,3}, Christian Ghiglione^{1,2,3} and Stéphane Noselli^{1,2,3,*}

ABSTRACT

When exposed to nutrient challenge, organisms have to adapt their physiology in order to balance reproduction with adult fitness. In mammals, ovarian follicles enter a massive growth phase during which they become highly dependent on gonadotrophic factors and nutrients. Somatic tissues play a crucial role in integrating these signals, controlling ovarian follicle atresia and eventually leading to the selection of a single follicle for ovulation. We used *Drosophila* follicles as a model to study the effect of starvation on follicle maturation. Upon starvation, *Drosophila* vitellogenic follicles adopt an 'atresia-like' behavior, in which some slow down their development whereas others enter degeneration. The mitotic-to-endocycle (M/E) transition is a critical step during *Drosophila* oogenesis, allowing the entry of egg chambers into vitellogenesis. Here, we describe a specific and transient phase during M/E switching that is paused upon starvation. The Insulin pathway induces the pausing of the M/E switch, blocking the entry of egg chambers into vitellogenesis. Pausing of the M/E switch involves a previously unknown crosstalk between FoxO, Cut and Notch that ensures full reversion of the process and rapid resumption of oogenesis upon refeeding. Our work reveals a novel genetic mechanism controlling the extent of the M/E switch upon starvation, thus integrating metabolic cues with development, growth and reproduction.

KEY WORDS: dFoxO, M/E switch, *Drosophila*, Follicle, Oogenesis

INTRODUCTION

Nutrient sensing is essential to coordinate growth and development during organogenesis. The conserved Insulin/Insulin-like growth factor (IIS) and Target of rapamycin (TOR) signaling pathways play a central role in coupling growth with nutrition in *Drosophila* (Edgar, 2006; Andersen et al., 2013). The TOR pathway controls cell-autonomous growth downstream of amino acids (Wang and Proud, 2009), whereas the IIS pathway acts as a systemic regulator. Under the conditions of a protein-rich diet, *Drosophila* insulin-like peptides (Dilps) secreted from the brain directly activate the Insulin receptor homolog (InR) in peripheral tissues to control metabolism, stress response, lifespan and reproduction (Brogiolo et al., 2001; Ikeya et al., 2002). Signaling downstream of InR involves PI3K and AKT, leading to the phosphorylation and subsequent cytoplasmic retention of the Forkhead transcription factor FoxO (Puig et al., 2003). On a protein-poor diet Dilp secretion is blocked (Géminard et al., 2009; Grönke et al., 2010), which leads to reduced InR

signaling and subsequent translocation of FoxO into the nucleus of target tissues, where it acts as a growth inhibitor.

During prolonged nutritional stress, the IIS and TOR pathways interact to adjust development and growth rates according to nutrient availability, allowing proper organ development (Colombani et al., 2003). However, the effects of transient diet change on organ development remain poorly understood. To study this question, we used oogenesis as a model to investigate how the high-energy-consuming egg chambers cope with nutrient variations, to which animals are submitted in the wild.

Egg chambers are composed of a cyst of 16 germline cells (1 oocyte and 15 nurse cells) surrounded by a single layer of somatic follicle cells (Fig. 1A). These two cell lineages originate, respectively, from germline and follicle stem cells, which are both present in the germarium. When flies are grown on a protein-rich medium, egg chambers are produced unceasingly, leading to the formation of regular strings of eggs of all developing stages (1 to 14) assembled into ovarioles. Two main phases of egg chamber development are distinguishable based on the follicle cell nuclear cycle: (1) a mitotic (M) phase from stages 1 to 6; and (2) an endocycle (E) phase (genomic DNA replication without cell division) from stages 7 to 10. During the mitotic phase, follicle cells are immature and express the homeobox transcription factor Cut (Fig. 1A,B,E) (Sun and Deng, 2005). Then, between stages 6 and 7, follicle cells switch their cell cycle program, exiting the mitotic cycle and entering the endocycle (Deng et al., 2001; Lopez-Schier and St Johnston, 2001; Tamori and Deng, 2013). This transition is known as the mitotic-to-endocycle (M/E) switch. This switch is under the control of the evolutionarily conserved Notch (N) signaling pathway (Deng et al., 2001; Lopez-Schier and St Johnston, 2001; Schaeffer et al., 2004; Shcherbata et al., 2004). N activation induces expression of the zinc-finger transcription factor Hindsight (Hnt; Pebbled – FlyBase), which in turn inhibits cut expression (Fig. 1A-E) (Sun and Deng, 2007). Cut downregulation is necessary and sufficient to promote entry into the endocycle, allowing follicle cell differentiation and maturation (Sun and Deng, 2005). At stage 8, N activity eventually returns to basal levels (Fig. 1B,C) (Sun et al., 2008).

The mitotic and endocycle phases roughly correspond to the early and vitellogenic phases of egg chamber development, respectively. These two phases have previously been shown to behave differentially upon starvation (Drummond-Barbosa and Spradling, 2001). During the early mitotic phase, starvation causes microtubule reorganization (Shimada et al., 2011) and germline and follicle cell division rates and growth slow down, leading to a developmental delay (LaFever and Drummond-Barbosa, 2005) as well as triggering the loss of germline stem cells in the germarium (Hsu et al., 2008; Hsu and Drummond-Barbosa, 2009, 2011; Yang et al., 2013). Mutations in *InR* reduce follicle cell proliferation, whereas some *Tor* mutations extend the mitotic phase (LaFever et al., 2010). By contrast, starvation during the endocycle phase triggers egg chamber degeneration (Drummond-Barbosa and Spradling, 2001; Pritchett and McCall,

¹Université Nice Sophia Antipolis, Institut de Biologie Valrose, iBV, Nice 06100, France. ²CNRS, Institut de Biologie Valrose, iBV, UMR 7277, Nice 06100, France. ³INSERM, Institut de Biologie Valrose, iBV, U1091, Nice 06100, France.

*Author for correspondence (noselli@unice.fr)

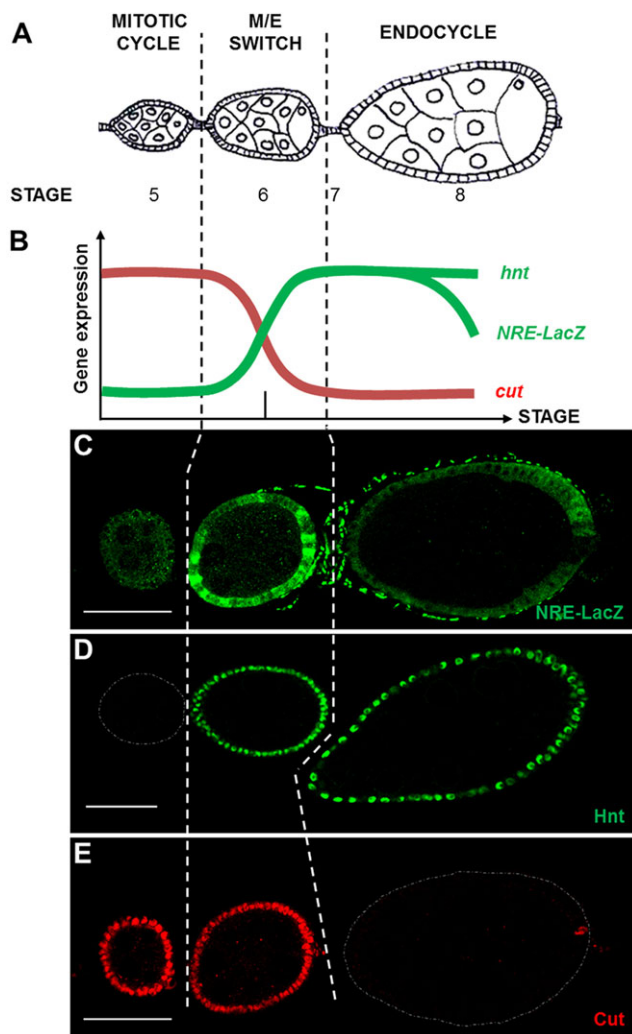


Fig. 1. Marker and gene expression profiles during the M/E switch. (A) Schematic representation of a *Drosophila* ovariole showing egg chambers before (stage 5), during (stage 6) and after (stage 8) the M/E switch. (B) Scheme showing the expression of *cut*, *NRE-lacZ* and *hnt* in follicle cells during the M/E switch. (C-E) Expression of NRE-lacZ (C), Hnt (D) and Cut (E) in egg chambers from control flies raised on a protein-rich medium. The stage 6 egg chambers undergoing the M/E switch are characterized by transient concomitant expression of Cut and N activity markers (NRE-lacZ and Hnt). NRE-lacZ shows a patchy expression pattern. Scale bars: 50 μm.

2012) in addition to a delayed growth rate (Drummond-Barbosa and Spradling, 2001; Ikeya et al., 2002; Tu et al., 2002; Richard et al., 2005; Schiesari et al., 2011). These observations reflect a sharp change in the survival/developmental response to nutrient shortage occurring at the M/E switch. Yet, the effects of starvation and the role of IIS during this important transition remain unknown.

In this study, we characterized the egg chamber response to nutrient variations specifically during the M/E transition. We show that nutrient deprivation stalls stage 6 egg chambers in a previously uncharacterized state that we term the ‘paused M/E switch’ (paused MES). We show that paused MES is reversible, with oogenesis resuming remarkably quickly following refeeding of starved flies. Paused MES is induced by a reduction of InR signaling. FoxO is dispensable for the normal M/E switch; however, it is essential for paused MES induction. In these conditions, FoxO activates Cut expression cell-autonomously in follicle cells, which maintains N in a paused MES-specific regulatory loop. Altogether, these results reveal

that upon starvation the M/E switch is paused, preserving the coupling between growth and development. This FoxO-dependent process enables prompt and efficient adaptation to nutrient supplies, thereby contributing to maintaining the balance between reproduction and nutrient availability.

RESULTS

Starvation induces a paused MES state

The M/E switch is a rapid transition that takes place in egg chambers at the end of stage 6, lasting ~3 h under normal conditions (Lin and Spradling, 1993). It has been characterized by N activation at the end of stage 6, followed by the loss of Cut at stage 7 (Sun and Deng, 2005). We performed a detailed analysis of the switch using (1) egg morphology, (2) the expression of Cut, which stains mitotic egg chambers, and (3) N signaling pathway reporters (NRE, Notch reporter element) that mark endocycling egg chambers (NRE>GFP or NRE-lacZ) (Fig. 1C,E) (Furriols and Bray, 2001; Zeng et al., 2010). Results show that the switch proceeds through an intermediate step between stages 6 and 7, during which follicle cells co-express N activity reporters (NRE-lacZ), Hnt and Cut (Fig. 1; supplementary material Fig. S1A). Statistical analysis shows that this intermediate stage lasts for ~2 h (supplementary material Table S1). Therefore, there is a specific and transient phase during which markers of the mitotic and endocycle phases show overlapping expression. Hereafter, we refer to this intermediate stage as the M/E switch (MES) stage. The Hnt and Cut markers suggest that MES stage egg chambers are in between cell cycle programs. We assessed the cell cycle state of MES cells and found that they exhibit neither mitotic (CycB, String-lacZ, phosphorylated Histone H3) nor endocycle (Fizzy related-lacZ, EdU incorporation) markers; hence, they are blocked exactly at the transition between the mitotic and endocycle phases (supplementary material Fig. S1).

To analyze MES behavior during starvation, we first verified that MES stage egg chambers showed the same overlapping Cut and NRE expressions (Fig. 2A,B) and intermediate cell cycle state (supplementary material Fig. S2). Next, we took advantage of the GAL80^{ts} system to pulse label newly generated MES stage egg chambers with GFP (McGuire et al., 2003). Briefly, fed or starved NRE>GFP flies were raised for 24 h at 29°C (a temperature permissive for GFP expression) in order to label egg chambers from MES stage onwards. Then, the egg chambers were shifted to a restrictive temperature (20°C) for 24 h to stop *de novo* GFP expression (Fig. 2F; see Materials and Methods). The MES stage was determined by the expression of NRE>GFP and Cut (Fig. 2C,D).

These experiments show that upon starvation MES egg chambers are paused, with the percentage of MES egg chambers increasing with time (supplementary material Fig. S2E). Indeed, there were no GFP-labeled MES stage egg chambers from control fed flies (Fig. 2C-C',E), with GFP being expressed in later, stage 8 egg chambers indicating that oogenesis proceeded normally. By contrast, most starved MES stage egg chambers were still labeled with GFP (Fig. 2D-D',E), indicating retention at the MES stage. We conclude that upon starvation MES stage egg chambers are maintained in the paused MES state.

MES pausing is a reversible process upon refeeding

Next, we analyzed the effect of refeeding on starvation-induced paused MES egg chambers. Flies were starved on poor medium to induce paused MES and then re-fed during different periods to test the ability of the paused egg chambers to proceed through the M/E switch once food was available again (Fig. 3A; see Materials and Methods). Egg chambers were marked using GFP flip-out clones

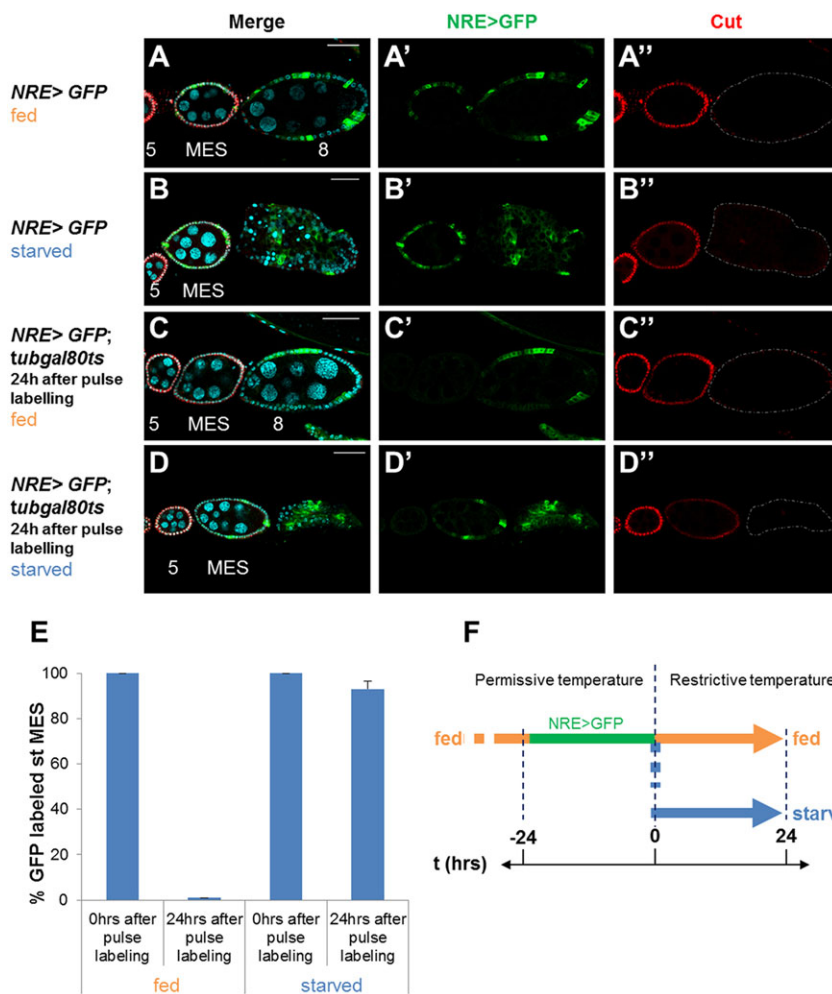


Fig. 2. Starvation blocks oogenesis in a paused MES state. (A-B'') NRE>GFP egg chambers from normally fed (A-A'') or starved (B-B'') flies. In starvation conditions, one of two endocycle egg chambers (expressing only NRE>GFP) is degenerating (B-B''). (C-D'') Pulse labeling of MES stage and later egg chambers (using NRE>GFP; *tubgal80^{ts}*) from fed (C-C'') and starved (D-D'') flies. Egg chambers were dissected 24 h after the shift from permissive (29°C) to restrictive (20°C) temperature to block *de novo* expression of GFP. MES stage egg chambers from control flies (C-C'') proceeded through the M/E switch, whereas those from starved flies did not (D-D''). Egg chambers are labeled with NRE>GFP (A'-D'') or Cut (A''-D''). Downregulation of Notch activity from stage 8 onwards is not detectable with the NRE>GFP reporter due to GFP perdurance. (E,F) The percentage of pulse-labeled MES stage egg chambers from fed and starved flies 24 h after chasing (shift from permissive to restrictive temperature, F). In fed flies, MES stage egg chambers proceeded normally through the M/E switch, whereas in starved flies they stalled. Data are the mean of duplicate experiments with s.d. $n \geq 200$ for each experiment. Scale bars: 50 μ m.

before starvation, in order to make sure that they experienced the full protocol (Fig. 3A; supplementary material Fig. S3A). To characterize the ability of paused MES to enter the endocycle, we measured the ratio of paused MES versus newly born non-degenerating stage 7-8 egg chambers. After 15 h of starvation (t_0 in Fig. 3), the proportion of MES stage relative to live stage 7-8 egg chambers increased compared with control fed flies (Fig. 3B,C), reflecting both the pausing of MES stage and degeneration of stage 7-8 egg chambers. Strikingly, after only 1 h of refeeding, we already observed full Cut downregulation in a significant proportion of GFP-positive stage 7-8 egg chambers, indicating that they had entered the endocycle (Fig. 3B,D,F,G). Increasing the refeeding period to 9 h allowed most MES egg chambers to develop into stage 8 egg chambers (Fig. 3B,E). After 24 h of rich food uptake, the ratio of MES/stage 7-8 was back to that of control fed flies (Fig. 3B).

Thus, upon nutrient supply, starvation-induced paused MES egg chambers are able to quickly revert to normal oogenesis by entering the endocycle. These data suggest that the M/E switch might serve as a nutritional checkpoint during oogenesis, responding rapidly to starvation and refeeding to allow processing through vitellogenesis.

IIS acts cell-autonomously in follicle cells to induce paused MES

The IIS pathway is known to mediate the response to starvation during development. In order to analyze the role of InR signaling in follicle cells during the M/E switch, we generated clones of

follicle cells mutant for different components of the IIS pathway: *InR*, the catalytic subunit of *PI3K* (*dp110*; *Pi3K92E* – FlyBase) and *akt* (*Akt1* – FlyBase) (Fig. 4A-C). All these conditions showed the same phenotype. Mutant follicle cells in otherwise wild-type endocycle egg chambers still expressed the mitotic stage marker Cut (Fig. 4A'''; data not shown), indicating that the mutant cells had not yet entered the endocycle (supplementary material Fig. S4). Consistently, mutant cells had smaller nuclei than their wild-type neighbors (Fig. 4A''-C'') and quantitative analysis of their DNA content indicated that they are diploid (supplementary material Fig. S4E). In addition, IIS pathway mutant cells showed N activation, as evidenced by the expression of Notch intracellular domain (N^{icd}), Hnt and NRE-lacZ (Fig. 4B''', C''', A''''-C''''; data not shown). Altogether, these results indicate that the reduction in N activity characteristic of stage 9 follicles had not occurred. Thus, IIS mutant follicle cells have all the features of paused MES cells.

In order to test whether activation of IIS is sufficient to force paused cells to proceed through the M/E switch, we generated IIS gain-of-function clones in starved egg chambers. In such conditions the expression of both Cut and NRE-lacZ was abolished, showing that ectopic IIS activity is sufficient to prompt follicle cells into progressing through the M/E switch regardless of the shortage of food supply (Fig. 4D-D''').

Altogether, these results show that the IIS pathway acts cell-autonomously in follicle cells to induce the paused MES state in response to starvation.

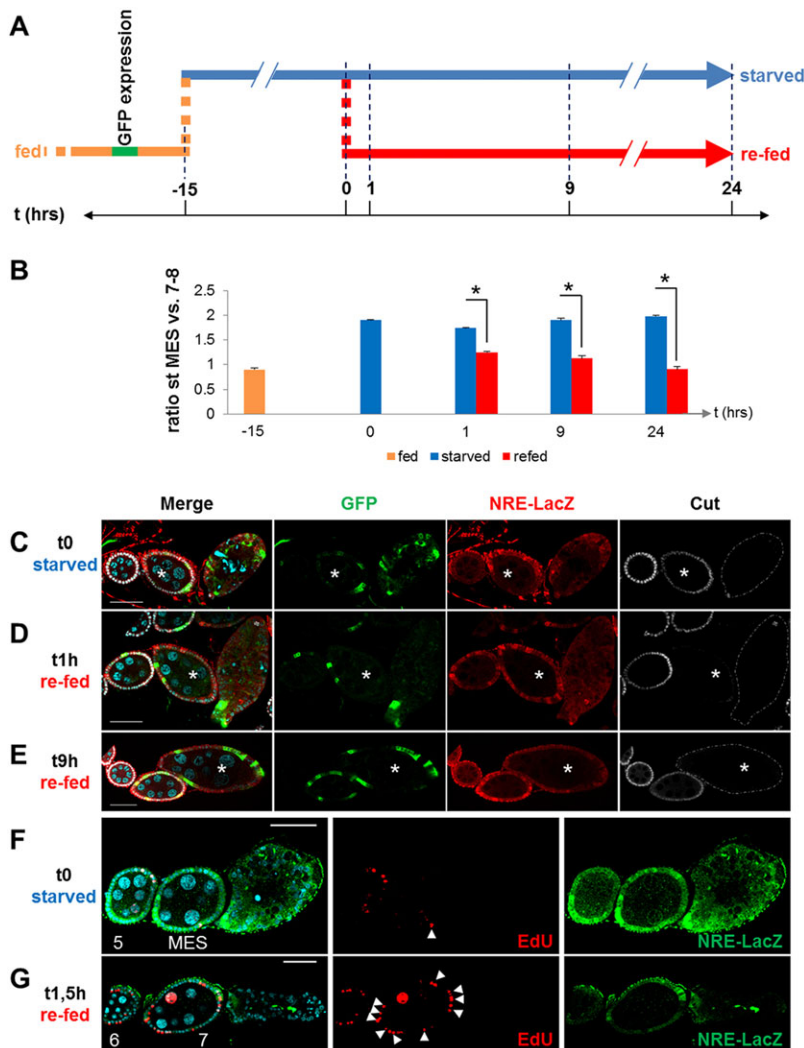


Fig. 3. The paused MES state is reversible upon refeeding. (A) Scheme of the refeeding experiment. Flies were starved for 15 h and the development of egg chambers analyzed 1, 9 or 24 h after refeeding. GFP expression allows the tracing of egg chambers that have gone through starvation. (B) The ratios between the number of MES stage and stage 7-8 egg chambers at different time points from control fed, starved or re-fed flies. $*P < 0.05$ (*t*-test); $n \geq 200$. (C-E) Expression of Cut, NRE-lacZ, GFP and DAPI (cyan) in egg chambers taken at different time points after refeeding (as indicated in A). Asterisks indicate paused MES egg chambers from starved flies (C) that developed onto stages 7 (D) and 8 (E) after refeeding. (F,G) Refeeding triggers entry into the endocycle. (F) Egg chambers from control flies starved for 24 h. (G) Egg chambers from flies starved for 24 h and re-fed for 1.5 h. Arrowheads indicate EdU incorporation in MES (F) and stage 7 (G) follicle cells. The MES egg chamber was identified using NRE-lacZ and Cut (data not shown). Scale bars: 50 μ m.

FoxO is essential to trigger paused MES upon starvation

It has been shown that reduction of the IIS pathway upon starvation leads to the translocation of the transcription factor FoxO to the nucleus, where it acts as a negative regulator of growth (Jünger et al., 2003; Puig et al., 2003). We were able to confirm that in fed flies, *InR* mutant follicle cells show high levels of nuclear FoxO, indicating that FoxO is activated cell-autonomously in response to loss of IIS function (Fig. 5A^{'''}). To test the role of FoxO in triggering the MES, we analyzed follicle cells mutant for *foxo*. In fed conditions, the levels of Cut and NRE-lacZ in *foxo* mutant cells were comparable to wild-type levels in both mitotic cycle and endocycle egg chambers (Fig. 5B-C^{'''}). These results indicate that, in the absence of nutritional stress, FoxO has no effect on the M/E switch, neither promoting nor delaying it.

To test whether FoxO is involved in generating starvation-induced paused MES, *foxo* ^{Δ 94} homozygous mutant flies were grown on poor medium and the MES/stage 7-10 ratio was measured (see Materials and Methods). In control heterozygous flies the ratio was doubled in poor diet conditions, reflecting the pausing of MES stages and leading to its increase compared with fed conditions (Fig. 5D). By contrast, in *foxo* ^{Δ 94} homozygous mutant flies, starvation no longer triggered MES pausing (Fig. 5D), indicating that FoxO is indeed required to induce paused MES in response to the lack of nutrients.

To verify that FoxO induces paused MES as a result of IIS downregulation, we generated clones of follicle cells that were mutant for *InR* or that overexpressed a dominant-negative form of PI3K. In either case, the loss of IIS function mimicked the starvation-induced paused MES state as shown by Cut misexpression (Fig. 5A-A^{'''}, E-E^{'''}). However, this phenotype was fully suppressed in the absence of FoxO (compare Fig. 5E-E^{'''} with 5F-F^{'''}), indicating that upon starvation IIS acts through FoxO to induce paused MES.

Finally, to assess whether FoxO is sufficient to induce paused MES, we generated clones overexpressing an active form of human FOXO3 [*hFOXO3a-TM*; mimicking FoxO gain-of-function (Jünger et al., 2003)] in the absence of any nutritional stress. Interestingly, activated human FOXO3 was able to induce the concomitant expression of Cut and NRE-lacZ (Fig. 5G-G^{'''}), indicating that FoxO is sufficient to trigger paused MES.

Altogether, these results indicate that, in the absence of nutritional stress, FoxO is dispensable for the formation of the MES. However, during starvation periods, FoxO plays a crucial role specifically at the M/E switch downstream of IIS, leading to the induction of paused MES egg chambers.

Cut activates Notch in a specific regulatory loop during paused MES

Paused MES egg chambers are characterized by a puzzling concomitant activation of Cut and N. Indeed, in normal egg

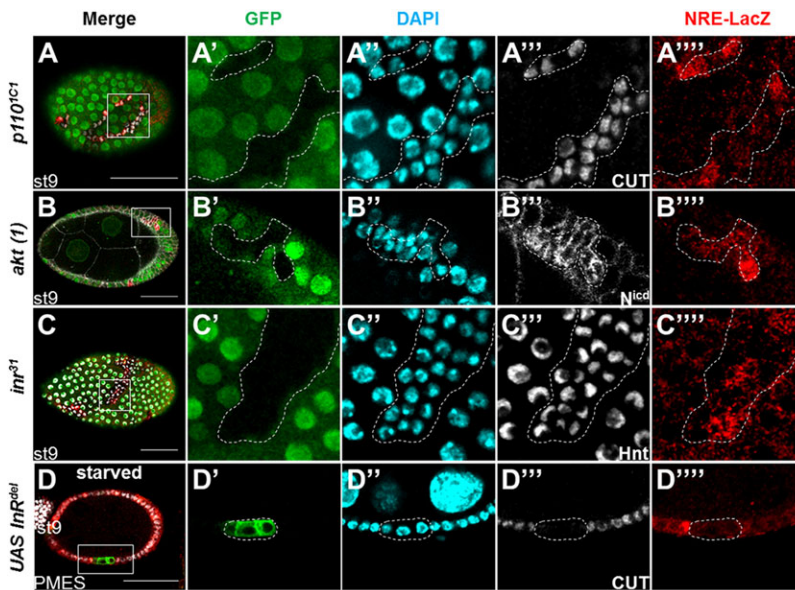


Fig. 4. IIS acts cell-autonomously in follicle cells to induce paused MES. (A-C^{'''}) IIS loss-of-function clones generated in stage 9 egg chambers. Mutant follicle cell clones are outlined and marked by the absence of GFP (A'-C'). (A-A^{'''}) Apical view of a *dp110*^{1C1} (*PI3K*) mosaic egg chamber. Mutant clones express Cut (A^{'''}). (B-B^{'''}) Transverse section of an *akt(1)* mosaic egg chamber. Mutant clones show stronger N^{icd} staining compared with wild-type cells (B^{'''}). (C-C^{'''}) Apical view of an *inr*²¹ mosaic egg chamber. Mutant clones show similar Hnt expression to wild-type cells (C^{'''}). (D-D^{'''}) Transverse section of a flip-out clone (marked by the presence of GFP, outlined) expressing UAS-dInR^{del} (activated form). Cut (D^{'''}) and NRE-lacZ (D^{''''}) expression is lost. The boxed regions in the merge are magnified in the single-channel images to the right. Scale bars: 50 μm.

chambers from MES stage onwards, a peak of N activity downregulates *cut* through Hnt and this is followed by a strong reduction of N activity (Fig. 1) (Sun and Deng, 2007; Sun et al., 2008). The paused MES-specific expression pattern therefore raises two questions: what maintains N activation and how is Cut expression preserved in the presence of N?

We first tested whether Cut could be the regulator of N during paused MES. We inhibited Cut expression in follicle cells while overexpressing the active form of human FOXO3 to mimic paused MES (>*hFOXO3a-TM*; *cut*^{RNAi}). Interestingly, loss of Cut activity led to the absence of both NRE-lacZ upregulation and N overexpression (Fig. 6A^{'''}, A^{''''}, compare with Fig. 5G^{'''}; supplementary material Fig. S5). These results suggest that Cut itself maintains N activity during the paused MES stage. To test whether Cut is sufficient to

maintain N, Cut was misexpressed in post-switch egg chambers. Ectopic Cut expression led to NRE-lacZ, N and Hnt upregulation (Fig. 6B-C^{'''}), indicating that Cut activates the N signaling pathway cell-autonomously. Furthermore, we found that N is essential for Cut-induced activation of N target genes. Indeed, upon N silencing Hnt is no longer activated by Cut (Fig. 6D-D^{'''}), indicating that N is epistatic to Cut on *hnt* regulation and that Cut does not regulate *hnt* directly.

We next analyzed the role of N in the paused MES regulatory pathway and in particular we tested whether N is also a negative regulator of *cut* in paused MES egg chambers. We made use of the IIS mutant paused MES egg chambers to overexpress the activated form of N (*N^{icd}*). N gain-of-function led to the absence of Cut upregulation (Fig. 6E-E^{'''}, compare with Fig. 4A and Fig. 5A; data

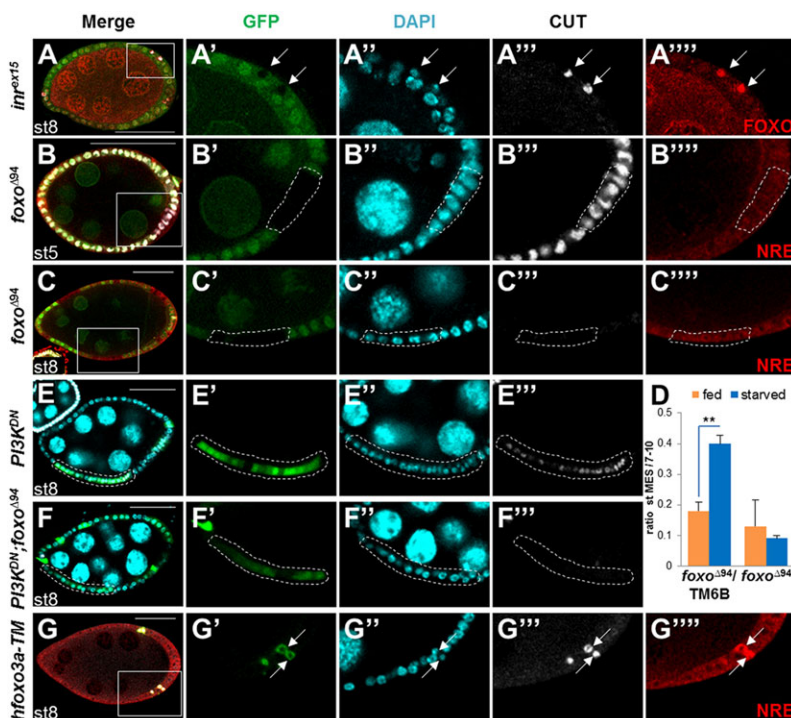


Fig. 5. FoxO is essential to trigger paused MES egg chambers. (A-A^{'''}) Endocycle (stage 8) *inr*^{ext15} mosaic egg chamber showing Cut expression (A^{'''}) and strong FoxO nuclear staining (A^{''''}) in mutant follicle cells. Mutant clones are marked by the absence of GFP (arrows). (B-C^{'''}) Mitotic (stage 5) (B) and endocycle (stage 8) (C) *foxo*^{Δ94} mosaic egg chambers showing similar stainings for Cut (B^{'''}-C^{'''}) and NRE-lacZ (B^{''''}-C^{''''}) in wild-type and mutant follicle cells (marked by the absence of GFP, outlined). (D) The ratio of MES/stage 7-10 egg chambers from fed or starved *foxo*^{Δ94} and control *foxo*^{Δ94}/*TM6B* flies. Data are the mean of duplicate experiments with s.d. ($n \geq 200$ in each experiment). ** $P < 0.01$ (*t*-test). (E-E^{'''}) Endocycle (stage 8) egg chamber with UAS-*p60(PI3K^{DN})*-expressing clones (marked by the presence of GFP, outlined), in which the expression of Cut is induced (E^{'''}). (F-F^{'''}) Endocycle (stage 8) egg chamber with UAS-*p60(PI3K^{DN})*; *foxo*^{Δ94} follicle cell clones (marked by the presence of GFP, outlined). Loss of *foxo* activity suppresses the expression of Cut (F^{'''}). (G-G^{'''}) Endocycle (stage 8) egg chamber containing UAS-*hFOXO3a-TM* follicle cell clones (marked by the presence of GFP, arrows). Ectopic activation of FoxO leads to Cut expression (G^{'''}) and upregulation of NRE-lacZ (G^{''''}). Loss-of-function (A-C), MARCM (E,F) or flip-out clones (G) are marked by the absence (green, A'-C') or presence (E'-G') of GFP, respectively. Egg chambers are marked with the clonal marker GFP (A'-C', E'-G'), DAPI staining (A'-C'', E'-G''), Cut (A^{'''}-C^{'''}, E^{'''}-G^{'''}), FoxO (A^{''''}) and NRE-lacZ (B^{''''}, C^{''''}, G^{''''}). The boxed regions in the merge are magnified in the single-channel images to the right. Scale bars: 50 μm.

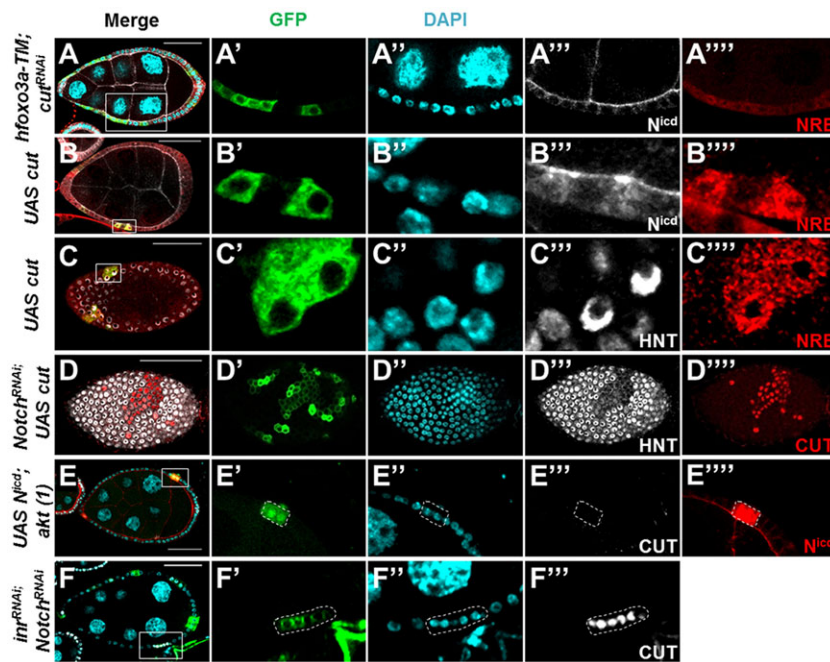


Fig. 6. Cut acts in a feedback loop to maintain Notch activity during paused MES. (A-A'') *UAS-hFOXO3a-TM*; *UAS-cut^{RNAi}* follicle cell clones (marked by the presence of GFP, A') show similar N^{icd} (A''), and NRE-lacZ (A''') staining as neighboring control cells. (B-C'') *UAS-cut* follicle cell clones (marked by the presence of GFP, B', C') show stronger N^{icd} (B''), Hnt (C'') and NRE-lacZ (B''', C''') staining compared with neighboring control cells. (D-D'') Loss of Hnt staining (D'') in *UAS-Notch^{RNAi}*; *UAS-cut* follicle cell clones (marked by the presence of GFP, D'). (E) Loss of Cut staining (E'') in *UAS-N^{icd}*; *akt(1)* follicle cell clones (marked by the presence of GFP, E'). (F) Cut expression is activated (F'') in *UAS-inr^{RNAi}*; *UAS-Notch^{RNAi}* follicle cell clones (marked by the presence of GFP, F'). Egg chambers are marked with GFP (A'-F'), DAPI staining (A''-F''), NRE-lacZ (A''''-C''''), N^{icd} (gray in A''', B'''; red in E'''), Hnt (C''', D''') and Cut (gray in E''', F'''; red in D'''). The boxed regions in the merge are magnified in the single-channel images to the right. Scale bars: 50 μ m.

not shown), suggesting that N also downregulates Cut in paused MES egg chambers, as it does during the normal M/E switch. This result was further confirmed in N loss-of-function conditions, which led to an increase in Cut expression (Fig. 6F-F'').

Altogether, these results reveal a regulatory loop characteristic of paused MES egg chambers that involves FoxO, Cut and N and leads to the concomitant activation of both Cut and N. In this pathway, N activity is maintained by Cut downstream of FoxO, while Cut levels are maintained by a balance between FoxO activator and N repressor. This regulatory network provides a molecular basis for the establishment of the paused MES state in starvation conditions (Fig. 7).

DISCUSSION

In the wild, adult organisms experience repeated sessions of nutrient challenge, forcing them to readapt. The IIS pathway contributes to the control of organ homeostasis and growth in response to such nutrient variations. In females, oogenesis represents a major source of energy consumption, competing with other physiological needs (Partridge et al., 2005). Investigating how IIS regulates ovarian development therefore provides insight into how an appropriate balance is maintained between homeostasis/survival and reproduction. To address this question, we used *Drosophila* egg chambers as a model of rapidly growing adult tissue with high nutrient requirements. Our work focused on the critical transition from early mitotic phases to vitellogenic stages.

Our data suggest that, upon starvation, the M/E switch may act as a nutritional checkpoint that is capable of restraining egg chamber progression into the energy-consuming vitellogenic stages, hence protecting developing eggs from starvation-induced degeneration. Paused MES maintenance relies on a particular regulatory pathway involving the activation of N by Cut, their concomitant activity being established through a specific regulatory loop (Fig. 7). The onset of paused MES is dependent on the loss of IIS signaling inducing Cut activation through FoxO, thereby linking nutrient levels to the state of oogenesis. Upon refeeding, cells respond quickly (within 1 h; Fig. 3) by downregulating FoxO and Cut, thus allowing oogenesis to resume through the 'unpausing' of the M/E switch (Fig. 7). Pausing egg

chamber development at the M/E switch thus provides a reactive and reversible mechanism to help control the flow of egg chambers towards vitellogenesis, as well as supplying a reservoir of preserved egg chambers that are ready to quickly resume oogenesis when nutritional conditions are favorable.

Depending on their stage of maturation, egg chambers behave differentially upon starvation. During early mitotic phase, prolonged nutrient deprivation and reduction of IIS activity slows egg chamber growth, which leads to a delay in egg maturation. Starvation during the later, vitellogenic stages induces progressive cell degeneration, a process that can be compared to vertebrate atresia (Hsueh et al., 1994).

Our results add a new step to the control of oogenesis upon nutrient challenge, participating in developmental delay. Indeed, pausing egg chamber development at the transition between the mitotic and endocycle phases is an ideal strategy to rapidly control the flow of egg chambers and prevent counterproductive and unnecessary energy expenditure when nutrients become limited. Altogether, the developmental delay that occurs during the mitotic phase combined with the paused MES state provide an efficient response to nutrient deprivation, preventing energy loss and protecting egg chambers from degeneration, as well as ensuring rapid oogenesis restart upon refeeding.

Induction of the paused MES state upon starvation relies on the maintenance of a specific regulatory loop involving the concomitant activity of Cut and N (Fig. 7), thus mimicking the normal M/E transition. The equilibrium between Cut and N activity depends on the balance between active nuclear FoxO and repressive N. Reduction of nuclear FoxO upon refeeding leads to disruption of the Cut/N equilibrium and subsequent progression through the M/E switch. A key aspect of the paused MES molecular pathway is the finding that Cut itself can maintain N at high levels. Therefore, Cut translates IIS activity into the N pathway, thus linking nutrient sensing and vitellogenesis. This association is likely to participate in setting a good balance between homeostasis/survival and reproduction, in register with nutrient availability.

The coupling of IIS with N signaling through Cut might represent a widespread means to link growth and other developmental/

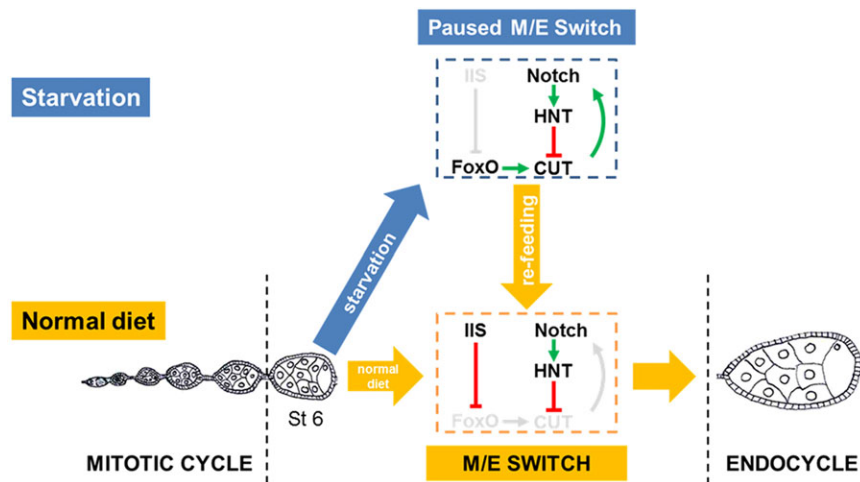


Fig. 7. The M/E switch pathway in normal and starvation conditions. The genetic pathway leading to the formation of paused MES egg chambers during starvation and its reversal to normal development upon refeeding. Paused MES maintenance involves the activation of N by Cut, their concomitant activity being established through a specific regulatory loop. The onset of paused MES is dependent on the loss of IIS signaling inducing Cut activation through FoxO. Upon refeeding, cells respond quickly by downregulating FoxO and Cut, thus allowing oogenesis to resume.

differentiation processes. In support of this view, previous work in *Drosophila* has shown an interaction between Cut and N during spiracle development (Pitsouli and Perrimon, 2013) and at the dorsoventral boundary of the wing disc pouch (Buceta et al., 2007). In addition, a FoxO/Fringe interaction in the germarium was also reported (Yang et al., 2013). Finally, work in vertebrates has demonstrated an interaction between the N and Insulin pathways in both physiological and developmental contexts, such as in the control of fatty acid metabolism in the liver (Pajvani et al., 2011), retinal neurogenesis (Jo et al., 2012), myogenic differentiation (Kitamura et al., 2007) and keratinocyte homeostasis (Mandinova et al., 2008). Future studies using *Drosophila* egg chambers should contribute to a better understanding of the complex interplay between the IIS and other signaling pathways in integrating metabolic cues with development, growth and differentiation.

MATERIALS AND METHODS

Drosophila strains and culture

Flies were grown on protein-rich medium (10 g/l agar, 17 g/l yeast extract, 82.5 g/l polenta, 60 g/l sugar with wet yeast paste). For starvation experiments, 2-day-old flies were switched from protein-rich medium to a 0.1× protein-poor medium (as above but with 1.7 g/l yeast extract and without wet yeast paste) during various periods of time (see figure legends). Two-day-old females were transferred to 29°C to induce somatic cell clones. The same procedure was used for flies expressing GAL4/UAS combinations to knockdown genes using RNAi or to express reporter lines.

The following *Drosophila* stocks were used: *Gbe-Su(H)-lacZ (NRE-lacZ)* (Furriols and Bray, 2001), *Gbe-Su(H)-Gal4 (NRE-Gal4)* (Zeng et al., 2010), *FRT82B dakt¹* (Rintelen et al., 2001), *FRT82B inr³¹* (Brogiolo et al., 2001), *UAS-dinr^{RNAi} RII2* (a gift from R. Ueda, NIG, Mishima, Japan), *UAS-N^{icd}* (Struhl et al., 1993), *UAS hFOXO3a-TM* (Jünger et al., 2003), *FRT82B dp110^{1C1}* [obtained from Hugo Stocker (Willecke et al., 2011)], *UAS cut⁵* (Krupp et al., 2005), *foxo^{Δ94}* and *FRT82B foxo^{Δ94}* (Slack et al., 2011), *FRT82B inr^{ex15}* (Song et al., 2003) and *string-lacZ (p[w+ stgB R6.4])* (a gift from B. Edgar, ZMBH, Heidelberg). *Tub-gal80^{ts}*, *UAS-rpr*, *UAS-dinr^{del}*, *UAS-cut^{RNAi} TRIP29625*, *UAS-N^{RNAi} TRIP28981*, *UAS-p60(PI3K^{DN})*, *fizzy related-lacZ* and *FRT82B* strains were from the Bloomington Stock Center.

Generation of mosaic clones

Mitotic clones were generated using the FLP/FRT technique (Xu and Rubin, 1993). Flies with mutant alleles recombined on *FRT82B* chromosomes were crossed to *hsFLP*; *FRT82B UbiGFP* flies. *UASp60*; *FRT82B foxo^{Δ94}* and *UASp60*; *FRT82B* flies were crossed to *yw, tubgal4-UAS GFP*; *FRT82B, tub gal80* flies (a gift from A. Ephrussi, EMBL, Heidelberg) to generate MARCM clones (Lee and Luo, 1999). Females with the required genotypes were heat shocked for 1 h at 37°C, twice a day for 3 days, and dissected 2 days later. Mosaic mutant clones were marked by the absence of GFP

(FLP/FRT) or by GFP expression (MARCM). Gain-of-function clones were generated using the flip-out technique by crossing flies to *hsFLP*; *act<CD2<gal4, UAS-GFP* (a gift from D. J. Montell, MCDB/UCSB, University of California, Santa Barbara). The progeny were heat shocked for 1 h at 37°C and dissected 1 or 2 days later or as indicated in the text.

TARGET technique and refeeding experiment

For the TARGET (McGuire et al., 2003) experiment, fed or starved *Gbe-Su(H)-Gal4, UAS GFP*; *tubgal80^{ts}* flies were raised for 24 h at 29°C to allow GFP expression, then switched to 20°C for 24 h. For the refeeding experiment, *hsFLP*; *act<CD2<gal4, UAS-GFP* flies were crossed to *Gbe-Su(H)-lacZ*. The progeny were fed for 2 days and heat shocked for 1 h at 37°C to induce GFP-expressing clones. Flies were then starved for 15 h and re-fed during different periods of time as indicated.

Scoring of MES stage egg chambers

The experiments described in Figs 3 and 5 were performed on separate occasions. Stage 7-10 egg chambers were scored in starved *foxo* homozygotes (Fig. 5D) because frequent morphological defects at vitellogenic stages made staging difficult. Although the ratios cannot be compared directly (due to a change in the denominator), the relative increase in MES is similar, with a doubling of MES (1 to 2 in Fig. 3 and 0.2 to 0.4 in Fig. 5). Furthermore, the percentage of MES versus stage 7-10 egg chambers was similar in the two conditions (9% in starvation conditions compared with 13% in homozygous *foxo* flies; data not shown).

Ploidy measurement

Flies were dissected, ovaries fixed and mounted in VECTASHIELD with DAPI (Vector Laboratories). Series of z-sections at 0.45 μm increments were acquired with a Zeiss LSM710 with 40× objective (zoom 7). Images were processed and analyzed using ImageJ (NIH). DAPI integrated density (intensity×area/cell) was scored for each nucleus. Nuclei from stage 5 and 6 egg chambers were used as diploid control cells and compared with *inr^{ex15}* mutant clones from stage 7-9 egg chambers. Results were analyzed using Student's *t*-test for non-parametric distributions ($n \geq 50$ for both control and mutant cells).

EdU labeling

Ovaries from fed or starved flies were quickly dissected in fresh PBS/EdU followed by a 1 h incubation in the same buffer before fixation. Staining was according to the manufacturer's protocol (Click-iT EdU Alexa Fluor Imaging Kit, Invitrogen).

Immunohistochemistry and microscopy

Antibody staining was carried out according to standard protocols. The following antibodies were used: mouse anti-Cut (1:100; 2B10, DSHB), rabbit anti-Cut (1:500; a gift from Y. N. Jan, UCSF, San Francisco), mouse anti-Hnt (1:100; 1G9, DSHB), mouse anti-Notch intracellular domain

(1:15; C17.9C6, DSHB), rabbit anti-FoxO (1:500; a gift from P. Léopold, iBV, Nice), chicken anti- β -galactosidase (1:1000; Gene Tex) and rabbit anti-cleaved Caspase 3 (1:200; Cell Signaling). The samples were mounted in VECTASHIELD with DAPI and analyzed by confocal microscopy using a Zeiss LSM510 or LSM710.

Acknowledgements

We thank R. Bodmer, S. Bray, W. M. Deng, A. Ephrussi, S. X. Hou, Y. N. Jan, P. Léopold, D. J. Montell, L. Partridge, L. Pick, H. Stocker, G. Struhl and R. Ueda for sharing reagents and fly lines; the TRiP at Harvard Medical School [NIH/NIGMS R01-GM084947] for transgenic RNAi fly stocks; the Bloomington Stock Center and Developmental Studies Hybridoma Bank (DSHB) for reagents; the iBV PRISM imaging facility for advice and support; the anonymous reviewers for their suggestions; and members of the laboratory and P. Léopold for discussion and comments.

Competing interests

The authors declare no competing financial interests.

Author contributions

P.J. and S.N. designed the experiments; P.J. and C.G. performed the experiments; and P.J. and S.N. wrote the manuscript.

Funding

Work in the S.N. laboratory is supported by Centre National de la Recherche Scientifique (CNRS), Agence Nationale de la Recherche (ANR), Fondation ARC pour la recherche sur le cancer and Fondation pour la recherche médicale (FRM). This work was funded by the French Government (ANR) through the 'Investments for the Future' LABEX SIGNALIFE [Program reference #ANR-11-LABX-0028-01].

Supplementary material

Supplementary material available online at <http://dev.biologists.org/lookup/suppl/doi:10.1242/dev.108399/-/DC1>

References

- Andersen, D. S., Colombani, J. and Léopold, P. (2013). Coordination of organ growth: principles and outstanding questions from the world of insects. *Trends Cell Biol.* **23**, 336-344.
- Brogio, W., Stocker, H., Ikeya, T., Rintelen, F., Fernandez, R. and Hafen, E. (2001). An evolutionarily conserved function of the *Drosophila* insulin receptor and insulin-like peptides in growth control. *Curr. Biol.* **11**, 213-221.
- Buceta, J., Herranz, H., Canela-Xandri, O., Reigada, R., Sagués, F. and Milán, M. (2007). Robustness and stability of the gene regulatory network involved in DV boundary formation in the *Drosophila* wing. *PLoS ONE* **2**, e602.
- Colombani, J., Raisin, S., Pantalacci, S., Radimerski, T., Montagne, J. and Léopold, P. (2003). A nutrient sensor mechanism controls *Drosophila* growth. *Cell* **114**, 739-749.
- Deng, W. M., Althausen, C. and Ruohola-Baker, H. (2001). Notch-Delta signaling induces a transition from mitotic cell cycle to endocycle in *Drosophila* follicle cells. *Development* **128**, 4737-4746.
- Drummond-Barbosa, D. and Spradling, A. C. (2001). Stem cells and their progeny respond to nutritional changes during *Drosophila* oogenesis. *Dev. Biol.* **231**, 265-278.
- Edgar, B. A. (2006). How flies get their size: genetics meets physiology. *Nat. Rev. Genet.* **7**, 907-916.
- Furriols, M. and Bray, S. (2001). A model Notch response element detects Suppressor of Hairless-dependent molecular switch. *Curr. Biol.* **11**, 60-64.
- Géminard, C., Rulifson, E. J. and Léopold, P. (2009). Remote control of insulin secretion by fat cells in *Drosophila*. *Cell Metab.* **10**, 199-207.
- Grönke, S., Clarke, D.-F., Broughton, S., Andrews, T. D. and Partridge, L. (2010). Molecular evolution and functional characterization of *Drosophila* insulin-like peptides. *PLoS Genet.* **6**, e1000857.
- Hsu, H.-J. and Drummond-Barbosa, D. (2009). Insulin levels control female germline stem cell maintenance via the niche in *Drosophila*. *Proc. Natl. Acad. Sci. USA* **106**, 1117-1121.
- Hsu, H.-J. and Drummond-Barbosa, D. (2011). Insulin signals control the competence of the *Drosophila* female germline stem cell niche to respond to Notch ligands. *Dev. Biol.* **350**, 290-300.
- Hsu, H.-J., LaFever, L. and Drummond-Barbosa, D. (2008). Diet controls normal and tumorous germline stem cells via insulin-dependent and -independent mechanisms in *Drosophila*. *Dev. Biol.* **313**, 700-712.
- Hsueh, A. J., Billig, H. and Tsafiri, A. (1994). Ovarian follicle atresia: a hormonally controlled apoptotic process. *Endocr. Rev.* **15**, 707-724.
- Ikeya, T., Galic, M., Belawat, P., Nairz, K. and Hafen, E. (2002). Nutrient-dependent expression of insulin-like peptides from neuroendocrine cells in the CNS contributes to growth regulation in *Drosophila*. *Curr. Biol.* **12**, 1293-1300.
- Jo, H. S., Kang, K. H., Joe, C. O. and Kim, J. W. (2012). Pten coordinates retinal neurogenesis by regulating Notch signalling. *EMBO J.* **31**, 817-828.
- Jünger, M. A., Rintelen, F., Stocker, H., Wasserman, J. D., Végh, M., Radimerski, T., Greenberg, M. E. and Hafen, E. (2003). The *Drosophila* forkhead transcription factor FOXO mediates the reduction in cell number associated with reduced insulin signaling. *J. Biol.* **2**, 20.
- Kitamura, T., Kitamura, Y. I., Funahashi, Y., Shawber, C. J., Castrillon, D. H., Kollipara, R., DePinho, R. A., Kitajewski, J. and Accili, D. (2007). A Foxo/Notch pathway controls myogenic differentiation and fiber type specification. *J. Clin. Invest.* **117**, 2477-2485.
- Krupp, J. J., Yaich, L. E., Wessells, R. J. and Bodmer, R. (2005). Identification of genetic loci that interact with cut during *Drosophila* wing-margin development. *Genetics* **170**, 1775-1795.
- LaFever, L. and Drummond-Barbosa, D. (2005). Direct control of germline stem cell division and cyst growth by neural insulin in *Drosophila*. *Science* **309**, 1071-1073.
- LaFever, L., Feoktistov, A., Hsu, H.-J. and Drummond-Barbosa, D. (2010). Specific roles of Target of rapamycin in the control of stem cells and their progeny in the *Drosophila* ovary. *Development* **137**, 2117-2126.
- Lee, T. and Luo, L. (1999). Mosaic analysis with a repressible cell marker for studies of gene function in neuronal morphogenesis. *Neuron* **22**, 451-461.
- Lin, H. and Spradling, A. C. (1993). Germline stem cell division and egg chamber development in transplanted *Drosophila* germlaria. *Dev. Biol.* **159**, 140-152.
- Lopez-Schier, H. and St Johnston, D. (2001). Delta signaling from the germ line controls the proliferation and differentiation of the somatic follicle cells during *Drosophila* oogenesis. *Genes Dev.* **15**, 1393-1405.
- Mandinova, A., Lefort, K., Tommasi di Vignano, A., Stonely, W., Ostano, P., Chiorino, G., Iwaki, H., Nakanishi, J. and Dotto, G. P. (2008). The FoxO3a gene is a key negative target of canonical Notch signalling in the keratinocyte UVB response. *EMBO J.* **27**, 1243-1254.
- McGuire, S. E., Le, P. T., Osborn, A. J., Matsumoto, K. and Davis, R. L. (2003). Spatiotemporal rescue of memory dysfunction in *Drosophila*. *Science* **302**, 1765-1768.
- Pajvani, U. B., Shawber, C. J., Samuel, V. T., Birkenfeld, A. L., Shulman, G. I., Kitajewski, J. and Accili, D. (2011). Inhibition of Notch signaling ameliorates insulin resistance in a FoxO1-dependent manner. *Nat. Med.* **17**, 961-967.
- Partridge, L., Gems, D. and Withers, D. J. (2005). Sex and death: what is the connection? *Cell* **120**, 461-472.
- Pitsouli, C. and Perrimon, N. (2013). The homeobox transcription factor cut coordinates patterning and growth during *Drosophila* airway remodeling. *Sci. Signal.* **6**, ra12.
- Pritchett, T. L. and McCall, K. (2012). Role of the insulin/Tor signaling network in starvation-induced programmed cell death in *Drosophila* oogenesis. *Cell Death Differ.* **19**, 1069-1079.
- Puig, O., Marr, M. T., Ruhf, M. L. and Tjian, R. (2003). Control of cell number by *Drosophila* FOXO: downstream and feedback regulation of the insulin receptor pathway. *Genes Dev.* **17**, 2006-2020.
- Richard, D. S., Rybczynski, R., Wilson, T. G., Wang, Y., Wayne, M. L., Zhou, Y., Partridge, L. and Harshman, L. G. (2005). Insulin signaling is necessary for vitellogenesis in *Drosophila* melanogaster independent of the roles of juvenile hormone and ecdysteroids: female sterility of the chico1 insulin signaling mutation is autonomous to the ovary. *J. Insect Physiol.* **51**, 455-464.
- Rintelen, F., Stocker, H., Thomas, G. and Hafen, E. (2001). PDK1 regulates growth through Akt and S6K in *Drosophila*. *Proc. Natl. Acad. Sci. USA* **98**, 15020-15025.
- Schaeffer, V., Althausen, C., Shcherbata, H. R., Deng, W.-M. and Ruohola-Baker, H. (2004). Notch-dependent Fizzy-related/Hec1/Cdh1 expression is required for the mitotic-to-endocycle transition in *Drosophila* follicle cells. *Curr. Biol.* **14**, 630-636.
- Schiesari, L., Kyriacou, C. P. and Costa, R. (2011). The hormonal and circadian basis for insect photoperiodic timing. *FEBS Lett.* **585**, 1450-1460.
- Shcherbata, H. R., Althausen, C., Findley, S. D. and Ruohola-Baker, H. (2004). The mitotic-to-endocycle switch in *Drosophila* follicle cells is executed by Notch-dependent regulation of G1/S, G2/M and M/G1 cell-cycle transitions. *Development* **131**, 3169-3181.
- Shimada, Y., Burn, K. M., Niwa, R. and Cooley, L. (2011). Reversible response of protein localization and microtubule organization to nutrient stress during *Drosophila* early oogenesis. *Dev. Biol.* **355**, 250-262.
- Slack, C., Giannakou, M. E., Foley, A., Goss, M. and Partridge, L. (2011). dFOXO-independent effects of reduced insulin-like signaling in *Drosophila*. *Aging Cell* **10**, 735-748.
- Song, J., Wu, L., Chen, Z., Kohanski, R. A. and Pick, L. (2003). Axons guided by insulin receptor in *Drosophila* visual system. *Science* **300**, 502-505.
- Struhl, G., Fitzgerald, K. and Greenwald, I. (1993). Intrinsic activity of the lin-12 and Notch intracellular domains in vivo. *Cell* **74**, 331-345.
- Sun, J. and Deng, W.-M. (2005). Notch-dependent downregulation of the homeodomain gene cut is required for the mitotic cycle/endocycle switch and cell differentiation in *Drosophila* follicle cells. *Development* **132**, 4299-4308.
- Sun, J. and Deng, W.-M. (2007). Hindsight mediates the role of notch in suppressing hedgehog signaling and cell proliferation. *Dev. Cell* **12**, 431-442.

- Sun, J., Smith, L., Armento, A. and Deng, W.-M.** (2008). Regulation of the endocycle/gene amplification switch by Notch and ecdysone signaling. *J. Cell Biol.* **182**, 885-896.
- Tamori, Y. and Deng, W.-M.** (2013). Tissue repair through cell competition and compensatory cellular hypertrophy in postmitotic epithelia. *Dev. Cell* **25**, 350-363.
- Tu, M.-P., Yin, C.-M. and Tatar, M.** (2002). Impaired ovarian ecdysone synthesis of *Drosophila melanogaster* insulin receptor mutants. *Aging Cell* **1**, 158-160.
- Wang, X. and Proud, C. G.** (2009). Nutrient control of TORC1, a cell-cycle regulator. *Trends Cell Biol.* **19**, 260-267.
- Willecke, M., Toggweiler, J. and Basler, K.** (2011). Loss of PI3K blocks cell-cycle progression in a *Drosophila* tumor model. *Oncogene* **30**, 4067-4074.
- Xu, T. and Rubin, G. M.** (1993). Analysis of genetic mosaics in developing and adult *Drosophila* tissues. *Development* **117**, 1223-1237.
- Yang, S.-A., Wang, W.-D., Chen, C.-T., Tseng, C.-Y., Chen, Y.-N. and Hsu, H.-J.** (2013). FOXO/Fringe is necessary for maintenance of the germline stem cell niche in response to insulin insufficiency. *Dev. Biol.* **382**, 124-135.
- Zeng, X., Chauhan, C. and Hou, S. X.** (2010). Characterization of midgut stem cell- and enteroblast-specific Gal4 lines in *Drosophila*. *Genesis* **48**, 607-611.

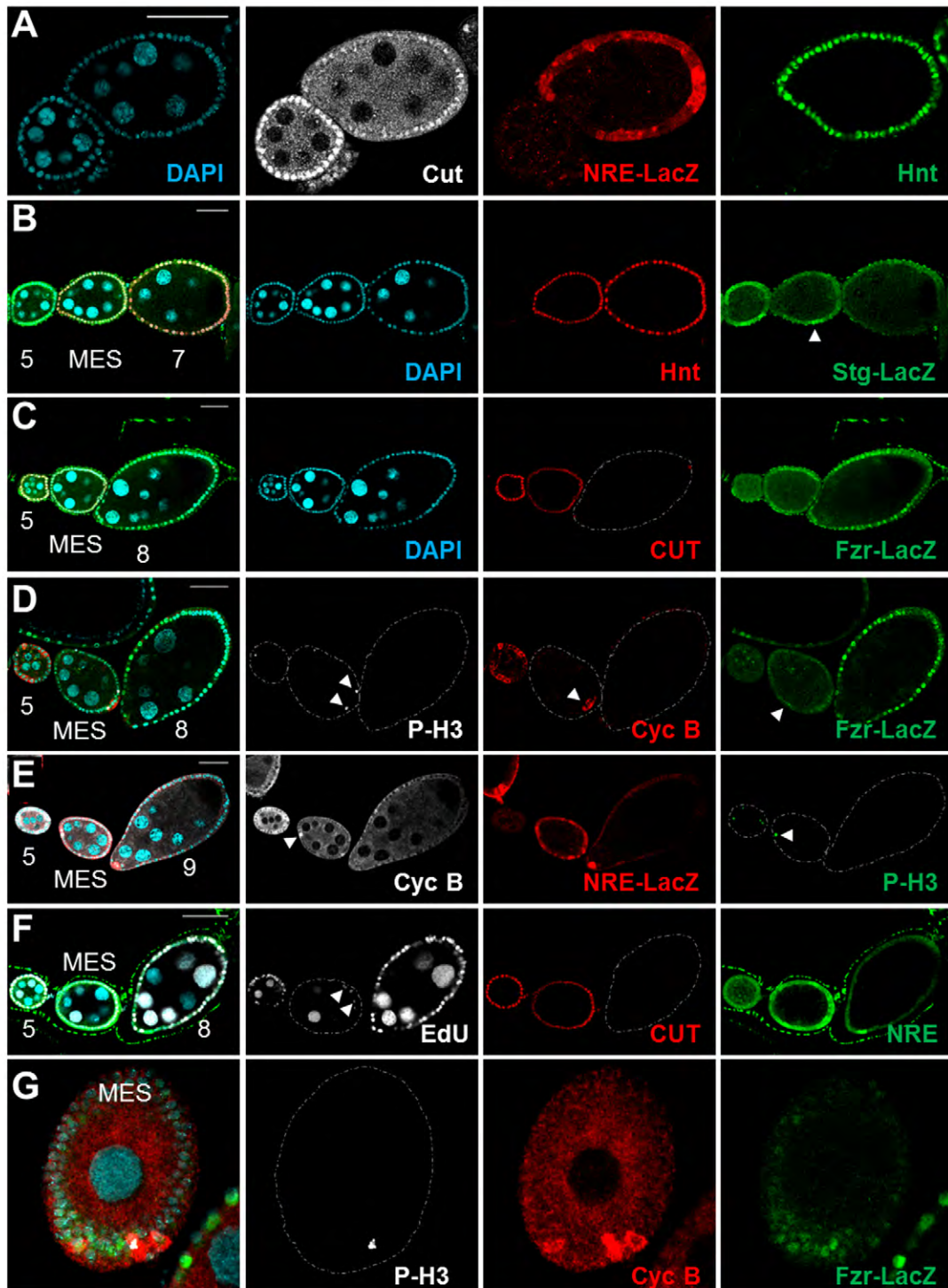


Fig. S1: Expression of mitotic and endocycle markers in MES cells.

All egg chambers are from normally fed flies. **A**) MES egg chambers show overlapping expression of the N activity reporter line NRE-LacZ (red) and of Hnt (green) and Cut (grey). DAPI (cyan). **B**) The arrowhead indicates Stg-LacZ expression in the MES egg chamber. DAPI (cyan), hnt (red) and Stg-LacZ (green). **C**) DAPI (cyan), Cut (red) and Fzr-LacZ (green). **D**) Arrowheads indicate P-H3, Cyclin B and Fzr-LacZ expressing cells in MES egg chambers. P-H3 (grey), Cyclin B (red) and Fzr-LacZ (green). **E**) Arrowheads indicate P-H3 and Cyclin B expressing cells in MES egg chambers. Cyclin B (grey), NRE-LacZ (red) and P-H3 (green). **F**) Arrowheads indicate EdU incorporation in a few cells from MES egg chambers. EdU (grey), Cut (red) and NRE-LacZ (green). **G**) Cyclin B (red), Fzr-LacZ (green) and P-H3 (grey). Scale bar: 50 μ m.

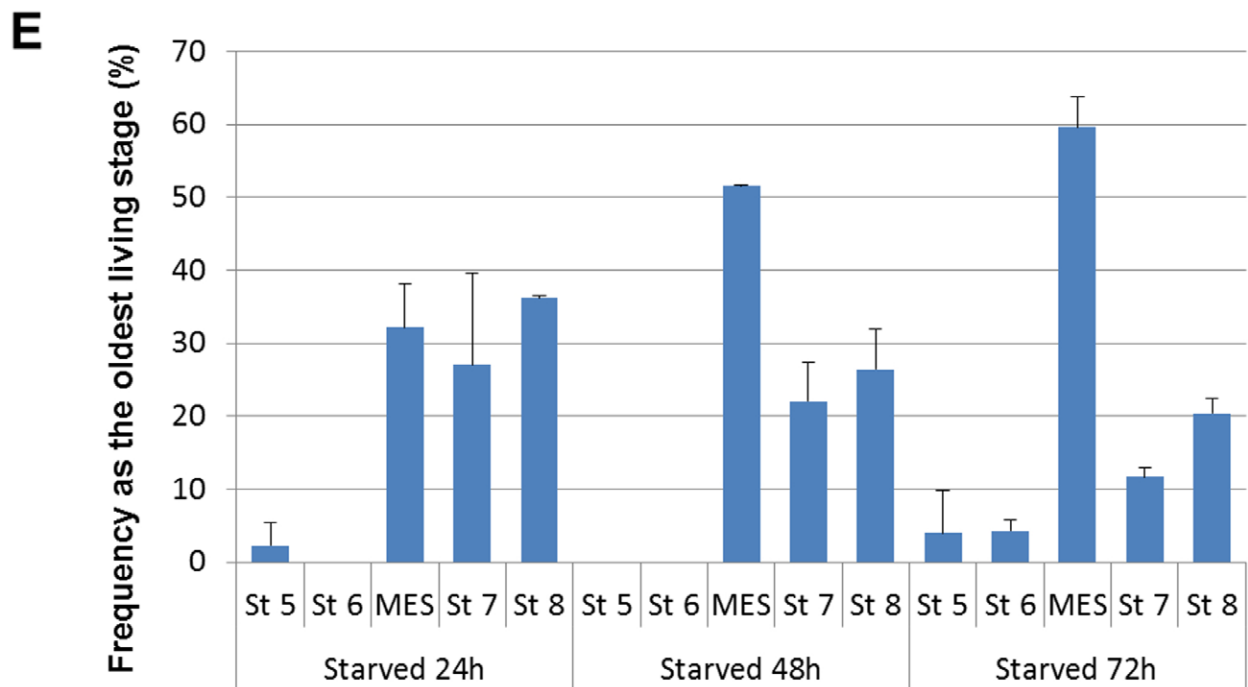
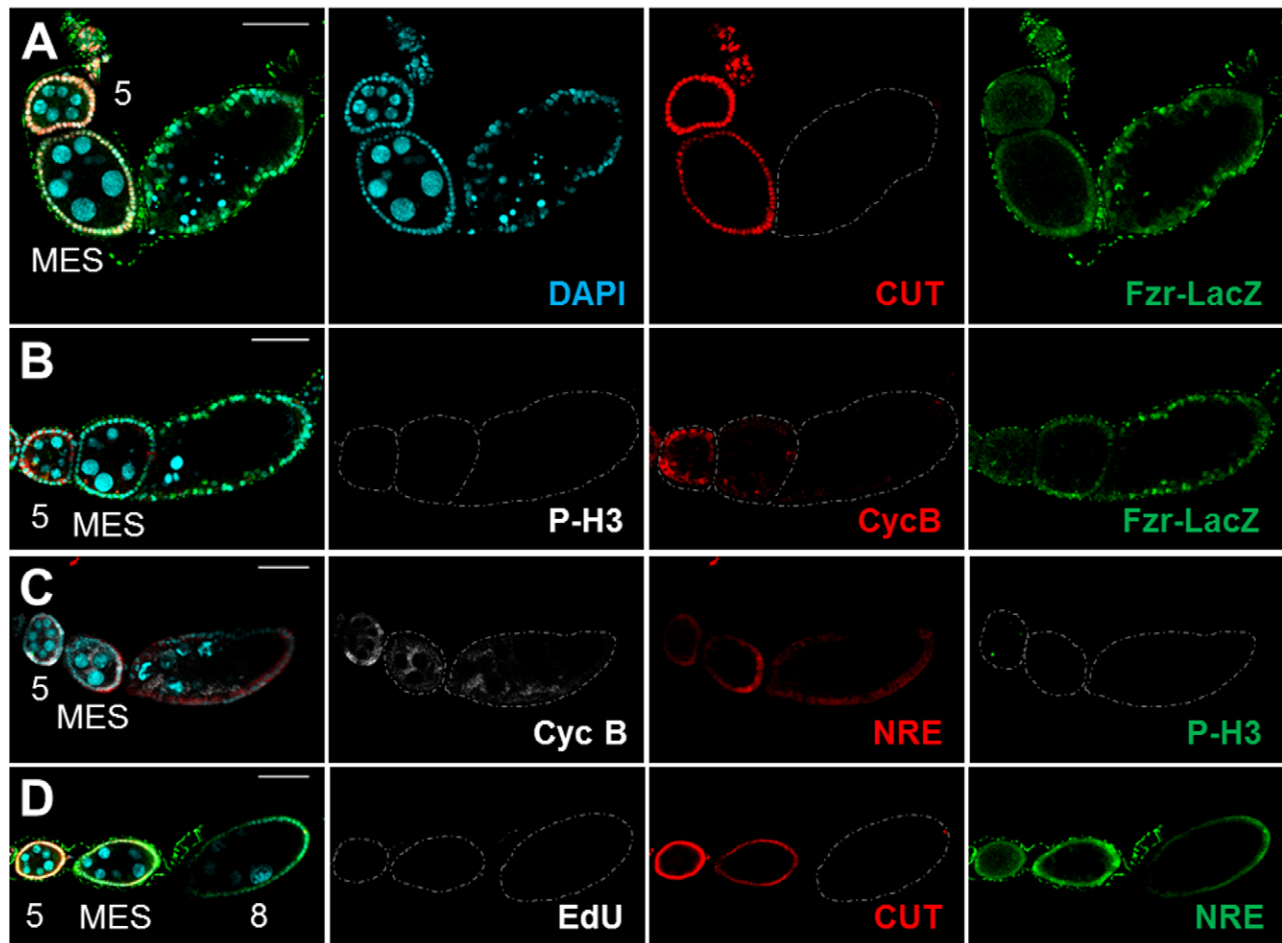


Fig. S2: Starvation-induced paused MES are in the same cell cycle state as MES.

All egg chambers are from flies starved for 24 hrs. **A**) DAPI (cyan), Cut (red) and Fzr-LacZ (green). **B**) P-H3 (grey), Cyclin B (red) and Fzr-LacZ (green). **C**) Cyclin B (grey), NRE-LacZ (red) and P-H3 (green). **D**) EdU (grey), Cut (red) and NRE-LacZ (green). **E**) Distribution of egg chambers occupying the last position before degenerating egg chambers. The results show a progressive increase in paused MES egg chambers over time. Scale bar: 50 μ m.

flip-out:UAS-GFP

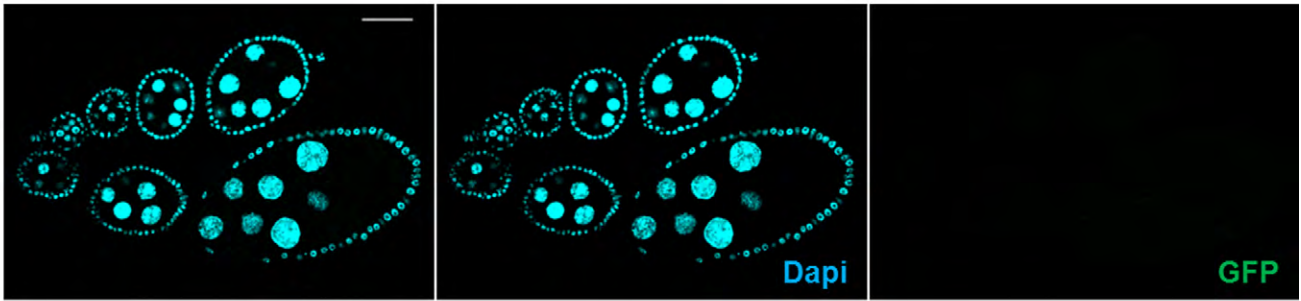


Fig. S3: Re-feeding triggers the entry into the endocycle.
The line used to generate flip-out clones (in Fig. 3) does not show leakiness.

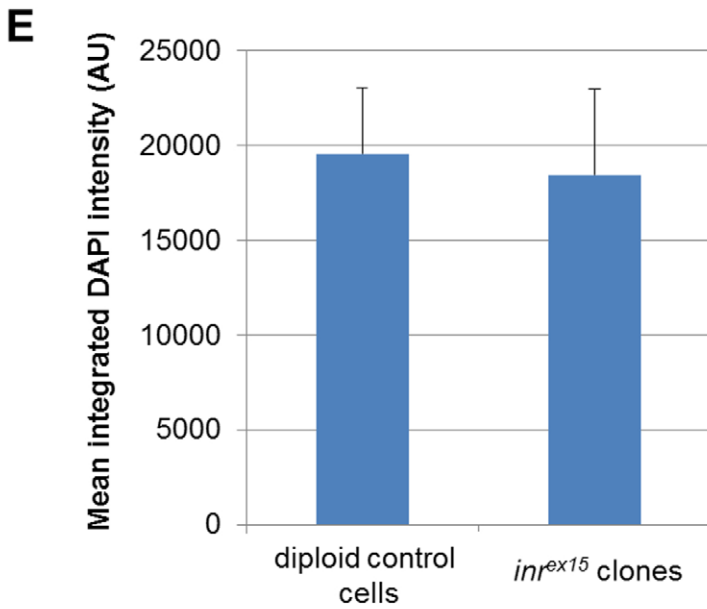
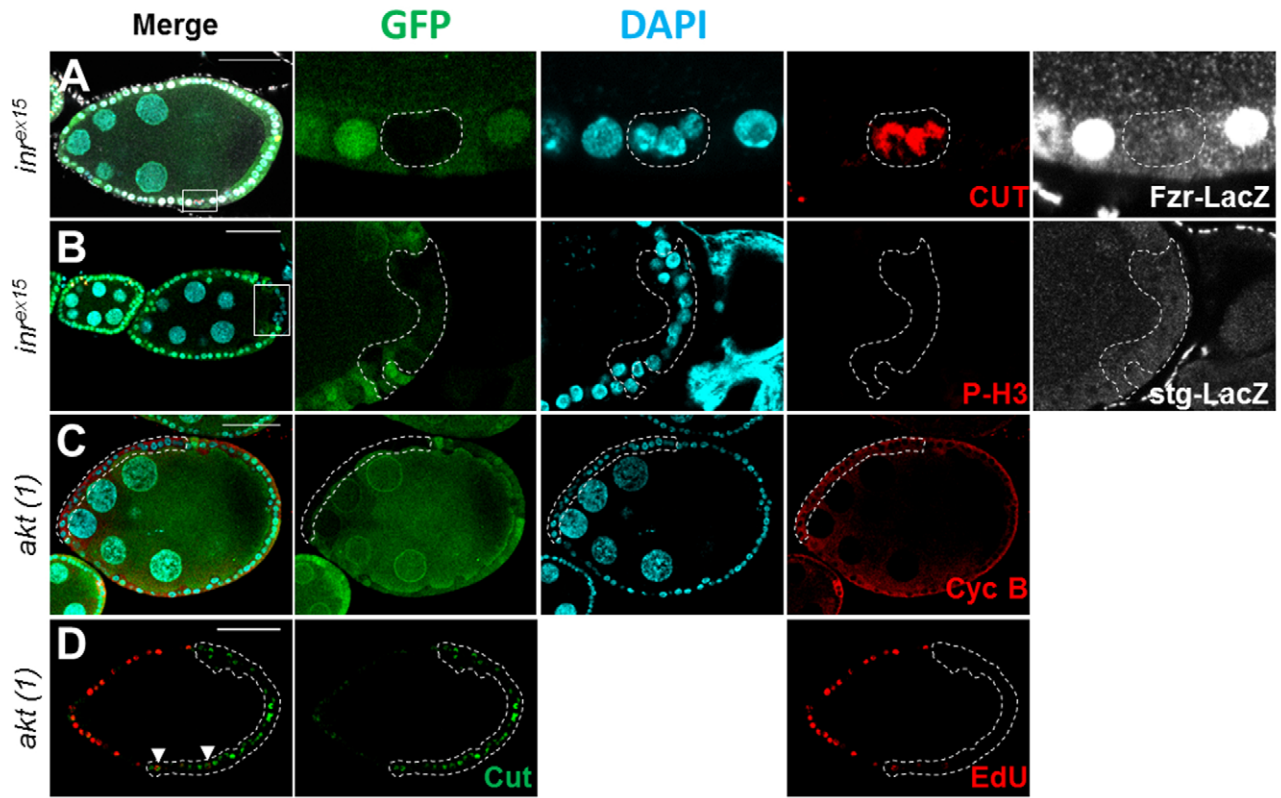


Fig. S4: Loss of function for IIS induces paused MES cells with intermediate cell cycle phenotype.

(A-D) Cross-section of *dinr* (A,B) and *dakt* (C,D) loss-of-function clones generated in stage 8 egg chambers. Mutant follicle cells are outlined and marked by the absence of GFP (green) or by Cut expression. Mutant clones are negative for *fzr-lacZ* (grey) (A), *stg-lacZ* (grey) and P-H3 (red) (B), CycB (red) (C). D) Some rare mutant cells show weak EdU (red) staining (arrow-head) and express Cut₁ (green). E) Histogram showing the integrated DAPI intensity from control diploid cells or from stage 7-9 egg chambers of *inr^{ex15}* mutant cells. The results show that they are not statistically different. $N \geq 50$, $P^{N.S.} = 0.166$. Scale bar: 50 μ m.

UAS: hfoxo^{3a}-TM; UAS: cut^{RNAi}

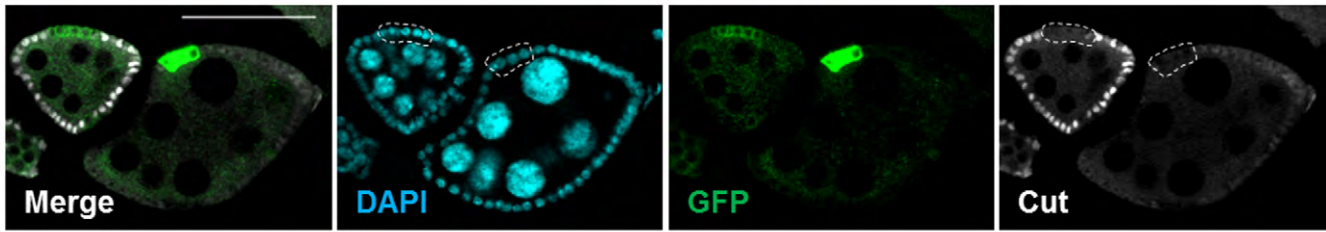


Fig. S5: Efficiency of *cut* RNAi silencing.

Cut expression in flip-out clones from stage 5 and 7 egg chambers expressing *cut* RNAi in a *foxo3A* (activating) background (*act<<gal4-UAS:GFP; UAS-hfoxo3a-TM; UAS-cut^{RNAi}*). DAPI (cyan), GFP (green), Cut (grey). Scale bar: 50 μ m.

Table S1: Determination of MES stage duration

	<i>n</i>	Frequency (%)	Duration (hrs)
Stage 5	230	48.5	5
MES stage	95	20	2

MES duration was estimated by its relative frequency compared with stage 5 within each ovariole (3 independent experiments, $n > 100$ in each experiment). Results show that MES are observed in 20% of ovarioles, compared with 48.5 % for stage 5 egg chambers (25°C; NRE>GFP/CyO genetic background). Therefore, the duration for MES is estimated at 2 hours, well consistent with the transient nature of MES.